Published in final edited form as:
J Immunol. 2010 July 15; 185(2): 1114–1123. doi:10.4049/jimmunol.1001143.

Innate retroviral restriction by Apobec3 promotes antibody affinity maturation *in vivo*[1]

Mario L. Santiago[*,†,‡], **Robert L. Benitez**[§], **Mauricio Montano**[§], **Kim J. Hasenkrug**[¶], and **Warner C. Greene**[§,#]

[*] Division of Infectious Diseases, University of Colorado Denver, 12700 E 19th Avenue, Mail Stop B168, Aurora, CO 80045

[†] Department of Microbiology, University of Colorado Denver, 12700 E 19th Avenue, Mail Stop B168, Aurora, CO 80045

[‡] Department of Immunology, University of Colorado Denver, 12700 E 19th Avenue, Mail Stop B168, Aurora, CO 80045

[§] Gladstone Institute of Virology and Immunology, University of California San Francisco, 1650 Owens Street, San Francisco, CA 94158

[#] Departments of Medicine, Microbiology and Immunology, University of California San Francisco, 1650 Owens Street, San Francisco, CA 94158

[¶] Rocky Mountain Laboratories, National Institutes of Allergy and Infectious Diseases, Hamilton, MT 59840

Abstract

Apobec3/*Rfv3* is an innate immune factor that promotes the neutralizing antibody response against Friend retrovirus (FV) in infected mice. Based on its evolutionary relationship to activation-induced deaminase (AID), Apobec3 might directly influence antibody class switching and affinity maturation independently of viral infection. Alternatively, the antiviral activity of Apobec3 may indirectly influence neutralizing antibody responses by reducing early FV-induced pathology in critical immune compartments. To distinguish between these possibilities, we immunized wild-type and Apobec3-deficient C57BL/6 (B6) mice with (4-hydroxy-3-nitrophenyl) acetyl (NP) hapten and evaluated the binding affinity of the resultant NP-specific antibodies. These studies revealed similar affinity maturation of NP-specific IgG1 antibodies between wild-type and Apobec3 deficient mice in the absence of FV infection. In contrast, hapten-specific antibody affinity maturation was significantly compromised in Apobec3-deficient mice infected with FV. In highly susceptible (B6 x A.BY)F_1 mice, the B6 Apobec3 gene protected multiple cell types in the bone marrow and spleen from acute FV infection including erythroid, B, T and myeloid cells. In addition, B6 Apobec3 deficiency was associated with elevated immunoglobulin levels but decreased induction of splenic germinal center B cells and plasmablasts during acute FV infection. These data suggest that Apobec3 indirectly influences FV-specific neutralizing antibody responses by reducing virus-induced immune dysfunction. These findings raise the possibility that enabling Apobec3 activity during acute infection with human pathogenic retroviruses such as HIV-1 may similarly facilitate stronger virus-specific neutralizing antibody responses.

[1]This work was supported by NIH grants R56 AI-0841230 to M.L.S. and R01 A065329 to W.C.G.

[*]To whom correspondence should be addressed: MARIO L. SANTIAGO, PhD, Division of Infectious Diseases, University of Colorado Denver, Mail Stop B168, 12700 E 19th Avenue, Aurora, CO 80045, Phone (303) 724 4946; Fax (303) 724 4926, mario.santiago@ucdenver.edu.

INTRODUCTION

The biological outcome of Friend retrovirus (FV) infection of mice is dictated by multiple resistance and susceptibility genes (1,2). FV infection of mouse strains such as A.BY and BALB/c results in the polyclonal activation of erythroblast precursors that leads to severe splenomegaly and erythroleukemia. On the other hand, mouse strains such as C57BL/6 (B6) are resistant to splenomegaly due to the absence of a dominant *Fv2* susceptibility gene (3,4). FV disease is also alleviated in certain mouse strains by the development of potent cell-mediated and humoral immune responses, both of which map to specific genetic loci. Cell-mediated immune responses are primarily controlled by the major histocompatibility complex (*H-2* locus) (5), while the neutralizing antibody response against FV is significantly influenced by a single autosomal dominant gene known as *Rfv3* (6). *Rfv3* resistant strains such as B6 produce stronger neutralizing antibody responses compared to *Rfv3* susceptible strains (A.BY, BALB/c), and this phenotype maps to a 60-gene region on chromosome 15 based on three consecutive studies of recombinant inbred mice (7–9).

We recently provided evidence that *Rfv3* is encoded by an innate restriction factor known as *Apobec3* (10). This conclusion was based on our demonstration that genetic inactivation of *Apobec3,* which is located within the 60-gene region on chromosome 15, reproduced the phenotype of an *Rfv3* susceptibility allele. Thus, (B6 *Apobec3*$^{-/-}$ x A.BY) F_1 mice developed weaker neutralizing antibody responses than (B6 *Apobec3*$^{+/+}$ x A.BY) F_1 mice assessed at 28 days post-infection (dpi) with FV. At high virus doses, even *Apobec3*-deficient B6 mice, which are resistant to splenomegaly, developed weaker neutralizing antibody responses against FV at 28 dpi compared to the corresponding wild-type mice.

Apobec3 encodes a deoxycytidine deaminase that, when incorporated into budding retroviral particles, can render these virions non-infectious in the next target cell [as reviewed in (11)]. Apobec3 can physically impede reverse transcription by its inherent binding to viral RNA (12,13), deaminate deoxycytidines in single-stranded DNA due to its enzymatic activity resulting in lethal G-to-A hypermutation in the viral plus strand (14–17), and/or impair viral integration through the formation of aberrant cDNA ends (18,19). *Rfv3* susceptible mouse strains (A.BY, BALB/c) exhibit decreased *Apobec3* mRNA expression (20,21), aberrant mRNA splicing of exon 2 (10), reduced *Apobec3* mRNA induction following infection (2) and destabilizing amino acid polymorphisms (21,22) that altogether, could compromise Apobec3 function. In addition, the alternatively spliced Apobec3 Δexon5 variant in the *Rfv3* resistant B6 strain was also shown to have stronger antiviral activity *in vitro* than full-length Apobec3 (21,22). Thus, a combination of these Apobec3 polymorphisms likely explains why Apobec3 is more potent in *Rfv3* resistant (B6) versus *Rfv3* susceptible (BALB/c, A.BY) strains. However, the underlying mechanism by which Apobec3 influences the adaptive immune response resulting in effective FV-specific neutralizing antibody responses remains unknown.

We previously proposed that the ability of Apobec3/*Rfv3* to influence the FV-specific neutralizing antibody response could be due either to a direct or indirect mechanism of action (10). Apobec3 is evolutionarily related to activation-induced deaminase (AID) (23), an enzyme expressed in B cells that facilitates class-switching and affinity maturation of antibodies (24). Thus, it is plausible that Apobec3 present in B cells could *directly* influence antibody development by supplementing AID function *in vivo*, even in the absence of virus infection. On the other hand, our group and others have shown that Apobec3 functions as an innate retroviral restriction factor *in vivo*, limiting the replication of Friend retrovirus (10,21), Moloney Murine Leukemia Virus (25) and Mouse Mammary Tumor Virus (26) before the onset of adaptive immune responses. These findings raise the possibility of an *indirect* mechanism of Apobec3 action, where the development of neutralizing antibody

responses are augmented as a result of Apobec3-mediated reduction in virus-induced pathology during the acute phase of infection.

To distinguish between these possibilities, we performed immunization studies in mice using a model hapten, (4-hydroxy-3-nitrophenyl) acetyl (NP). The NP-hapten immunization system has been used extensively to evaluate antibody affinity maturation (27–29). Thus, we monitored the affinity maturation of the resulting NP-specific antibodies in the presence or absence of FV infection. In addition, we characterized various immune compartments in the presence and absence of FV infection, looking for evidence of humoral immune dysregulation. Taken together, our data strongly support an indirect mechanism of Apobec3 action. These results raise the possibility that enabling Apobec3 function during acute infection may augment neutralizing antibody responses against a range of pathogenic human retroviruses including HIV-1.

MATERIALS AND METHODS

Mouse strains

C57BL/6 (B6) (*H-2*$^{b/b}$ *Fv2*$^{r/r}$ *Rfv3*$^{r/r}$), BALB/c (*H-2*$^{d/d}$ *Fv2*$^{s/s}$ *Rfv3*$^{s/s}$) and A.BY (*H-2*$^{b/b}$ *Fv2*$^{s/s}$ *Rfv3*$^{s/s}$) strains were purchased from The Jackson Laboratory. Apobec3-deficient mice, constructed using the XN450 gene-trap embryonic cell line (BayGenomics) were backcrossed for 8 generations in the B6 background (10). The mouse studies were performed in full accordance to UCSF and UCD institutional policies regarding animal care and use.

Real-time PCR

Erythroid, B, T, myeloid and dendritic cells were purified from B6 splenocytes and bone marrow cells using magnetic beads linked to antibodies against Ter119, CD19, CD90.2 (Thy1.2) and CD11c, respectively (Miltenyi Biotec). RNA from these cell subpopulations was extracted using the RNAEasy kit (Qiagen) and subjected to quantitative Taqman RT-PCR. The primers mA3.F (5′-CTGCCATGGACCTATACGAA) and mA3.R (5′-TCCTGAAGCTT AGAATCCTGGT) are located in exons 3 and 4 of *Apobec3* and amplify a 124 bp fragment. These primers, including the Taqman probe mA3.P (5′FAM-CCAAGGCCTGAATCGCCTGC-TAMRA-3′) are conserved between *Rfv3* resistant (B6) and susceptible (A.BY, BALB/c) strains. Total RNA (10 ng) was reverse-transcribed using with the mA3.F primer using the RT^2 reverse transcription kit (SABiosciences). Complementary DNA (cDNA) samples were subjected to quantitative PCR by mixing 2 μl of cDNA with 20 nM of mA3.F and mA3.R, 20 nM of mA3.P and 1x of the Taqman Universal Master Mix (Applied Biosciences) in a 22 μl reaction. The cycling conditions consisted of a hot-start activation step at 95°C for 15 min, followed by 40 cycles of 94°C for 15 s and 60°C for 60 s. Beta-actin levels were quantified using 10nM of mouse beta-actin primers (SA Biosciences, Catalogue No. PPM02945A), followed by quantitative PCR using SYBR green. Relative *Apobec3* mRNA levels were computed using a power equation (C_T vs. log quantity, r^2>0.98) based on an in-plate standard curve generated from serial dilutions of an Apobec3 expression plasmid with known copy number, and values were normalized against input beta-actin levels.

Hapten immunization

B6 *Apobec3*$^{+/+}$ and *Apobec3*$^{-/-}$ mice (>4 months old) and (B6 *Apobec3*$^{+/+}$ x BALB/c) F_1 and (B6 *Apobec3*$^{-/-}$ x BALB/c) F_1 (6–8 weeks old) mice were immunized intraperitoneally (i.p.) with 100 μg of NP conjugated to chicken gamma-globulin (NP_{26}-CGG) (Biosearch Technologies) in Imject alum (Pierce). Plasma samples were harvested 2 and 4 weeks after priming and boosting. In some experiments, the NP boost was preceded by infection with

7500 SFFU of FV stock. The plasma samples were subjected to an enzyme-linked immunosorbent assay (ELISA) using bovine serum albumin conjugated to low (NP_3 or NP_4) or high levels (NP_{33} or NP_{23}) of nitrophenyl hapten per molecule (Biosearch Technologies). Total NP-specific antibodies (both low- and high-affinity) are expected to bind CGG heavily substituted with NP, while only high-affinity NP-specific antibodies are expected to bind to CGG containing low level NP substitution. Thus, the ratio of the binding titers for the low versus the high-NP substituted CGG (or the "NP-reactivity ratio") provides a reliable measure of binding affinity. This approach was previously validated using a panel NP-specific monoclonal antibodies, which revealed a strong positive correlation between the NP-reactivity ratio and the binding affinity of the monoclonal antibodies to NP as measured by competitive radioimmunoassay (30), isothermal titration calorimetry (31) and surface plasmon resonance (32). Importantly, an increase in NP-reactivity ratio following NP-boosting is accompanied by increased somatic hypermutation of the VH186.2 locus from NP-specific B cells in germinal centers (27–29). Briefly, 100 ng of NP-BSA were coated into 96-well Immulon-4 plates overnight, followed by blocking for >2 hours with phosphate buffered saline containing 0.05% Tween-20 (PBS-T). Serial 10-fold dilutions of plasma in PBS were incubated at 37°C for 2 hours, washed 3x with PBS-T, then 1:50,000–1:250,000 dilution of goat anti-IgG1 conjugated to horseradish peroxidase (Bethyl) was incubated for 1 hour at 37°C. After 3 washes with PBS-T, the samples were developed using TMB substrate (Sigma) and stopped using 2N H_2SO_4. Absorbances were read at 450 nm and used to construct binding curves. The 50% binding concentrations were estimated graphically using Microsoft Excel. Relative binding affinities were estimated by dividing the 50% binding concentration against low-molar hapten (NP_3 or NP_4) over high-molar hapten (NP_{33} or NP_{23}) and multiplying these NP-reactivity ratios by 100.

FV infection

FV stocks were prepared and titered as previously described (6). The original FV stock that was used to describe (6), characterize (33,34), map (7–9) and molecularly identify (11,21) *Rfv3* contained three viruses: a replication-competent Friend Murine Leukemia virus, a replication-defective Spleen-Focus Forming Virus, and lactate dehydrogenase elevating virus (LDV), a positive-stranded RNA virus (35,36). Although an LDV-free virus stock exists, the LDV-plus stock was utilized to enable valid correlations with the historic *Rfv3* phenotype. The studies were performed on congenic B6 mice by default to ensure that Apobec3 is completely absent (*Rfv3* susceptible strains may still express residual Apobec3). However, the B6 strain is highly resistant to FV infection due to the $Fv2^{r/r}$ phenotype. Experiments aimed at directly evaluating FV infection, particularly by flow cytometry, were therefore performed in highly susceptible (B6 x A.BY)F_1 mice, a prototypic mouse strain used for studying FV immune responses, including the *Rfv3* phenotype (6). Mice (>4 months old, both males and females) were infected with 1400 (B6 x A.BY)F_1 or 7500 (B6) spleen focus forming units (SFFU) of virus intravenously. Spleen and/or bone marrow samples were harvested at 7 dpi and subjected to flow cytometry, while plasma samples were used for ELISA.

Flow cytometry

Bone marrow and splenocytes ($0.5–1.0 \times 10^6$ cells) were stained for 1 hr at 4°C with hybridoma supernatant from MAb34, which reacts with the surface Glyco-Gag protein of FV (35,37). The cells were washed once, then co-stained with goat anti-mouse IgG2b conjugated to APC (Columbia Biosciences). Other antibodies used to co-stain the cells included Ter119-PE (TER119), CD4-PE (RM4-5), CD8-FITC (53-6.7), GL7-FITC (Ly-77), CD138-PE (281-2), Gr1-PE (RB6-8C5), CD11b-PE (M1/70) (BD Biosciences); IgD-PE (11–26c.2a), CD19-PerCP-Cy5.5 (6D5), CD3-PerCP-Cy5.5 (17A2) (Biolegend) and B220-FITC (RA3.6B2), CD11c-FITC (N418), IgM-FITC (II/41) (eBioscience). The

corresponding isotype controls were included for gate construction. These antibodies were incubated with the cells for 30 min at 4°C. The samples were washed 3x in FACS buffer (PBS + 2% FBS), fixed with 0.5% paraformaldehyde in PBS and analyzed on a FACScalibur II (Becton Dickinson) flow cytometer with collection of 80,000–120,000 events per sample. Cell subpopulations were analyzed using Flowjo (TreeStar, Inc).

Measurement of immunoglobulin levels

The levels of total IgA, IgG, IgM, IgG1, IgG2b and IgG3 were measured using a commercial ELISA kit (ICL). The levels of these immunoglobulins were computed using an in-plate standard curve.

RESULTS

Relative expression of Apobec3 in immune cell subpopulations

Previous studies have shown that *Apobec3* mRNA is highly expressed in bone marrow and spleen, the primary sites of FV infection *in vivo* (38). However, *Apobec3* mRNA expression in specific cell subpopulations within these tissues has not been carefully analyzed. In particular, for Apobec3 to directly alter anti-FV somatic hypermutation and antibody affinity, Apobec3 must be expressed in B cells. Alternatively, an indirect mechanism of action requires expression of Apobec3 in at least one cell type targeted by FV. Of note, erythroid ($Ter119^+$) cells are primary targets of FV infection and may be principally responsible for generating the resultant viremia (39). We therefore measured *Apobec3* mRNA levels from magnetic bead-purified $Ter119^+$ erythroid, $CD19^+$ B, $CD3^+$ T cells and $CD11c^+$ dendritic cells using quantitiative real-time PCR. As shown in Figure 1, each of these cell types expressed *Apobec3* mRNA. B cells present in bone marrow and splenic tissue exhibited the highest levels of expression while erythroid cells expressed 2-fold more *Apobec3* than total bone marrow cells. This pattern of expression of *Apobec3* did not obviously favor either a direct or indirect mechanism of Apobec3/*Rfv3* action.

Normal antibody responses in Apobec3-deficient mice are significantly compromised in the context of FV infection

To evaluate whether Apobec3 directly influenced antibody responses by supplementing AID function *in vivo*, we performed immunization studies against a well-documented model immunogen, the 4-hydroxy-3-nitrophenyl (NP) acetyl hapten (Fig. 2A). NP consistently elicits a T-cell dependent IgG1 response that maps to the VH186.2 locus (27). This model system can be used to evaluate antigen-specific B cell development. For example, it has been shown that $AID^{-/-}$ mice do not mount an NP-specific IgG1 response (24). Furthermore, the binding affinity of NP-specific antibodies can be assessed using a well-established differential ELISA employing BSA conjugated to low- or high-molar levels of hapten (30). As expected, boosting NP-immunized mice with the NP hapten resulted in an increase in the relative binding affinity of NP-specific antibodies in B6 *Apobec3*$^{+/+}$ mice (Fig. 2B). However, an essentially overlapping affinity maturation response was observed in B6 *Apobec3*$^{-/-}$ mice (Fig. 2B). Similar data was also observed for (B6 *Apobec3*$^{+/+}$ x BALB/c)F_1 and (B6 *Apobec3*$^{-/-}$ x BALB/c)F_1 mice (Fig. 2C). These findings suggested that Apobec3 did not directly influence NP-specific IgG1 antibody affinity maturation *in vivo* and thus argue against a direct model for Apobec3/*Rfv3* action.

We next investigated whether Apobec3 influenced the NP-specific antibody response in the context of FV infection. NP-primed B6 mice (wild-type and *Apobec3*-deficient) were infected with FV three days prior to the NP boost (Fig. 3A). The binding affinity of NP-specific antibodies was estimated based on the ratio of 50% binding titers obtained with low- (NP_4) versus high-molar (NP_{23}) hapten. Similar to results in Fig. 2B, the binding

affinity of NP-specific antibodies was similar between wild-type and Apobec3-deficient mice 2 and 4 weeks following NP priming (not shown). However, the binding affinity of NP-specific antibodies in Apobec3-deficient mice was significantly lower 4 weeks following FV infection and NP boosting than observed in B6 mice expressing Apobec3 (Fig. 3B). These findings suggested that the innate restricting activities of Apobec3 could counteract the detrimental effects of FV infection on antibody affinity maturation. These results favor an indirect mechanism of Apobec3/*Rfv3* action.

Apobec3 protects multiple immune cell types from acute FV infection

Our prior data indicate that the presence of Apobec3 results in lower plasma viremia in FV-infected animals examined at 7 days post-infection (dpi) (10). Since restriction of virus levels occurred prior to the peak of adaptive immune responses, it was possible that Apobec3-mediated innate immune activity restricted FV replication in specific cell types in the bone marrow and spleen. Since infection of immune cells could impair their development and function, restriction of such infection by Apobec3 could potentially improve NP-specific antibody affinity maturation and virus-specific neutralizing antibody responses. To analyze infection of specific cell subsets, flow cytometry was used to detect the expression of a surface antigen of FV, Glycosylated Gag (Glyco-Gag), in conjunction with cellular subset-specific antigens. FV infection experiments were performed in the (B6 x A.BY)F_1 background that encode or do not encode the B6 Apobec3 gene. Due to the expression of the dominant *Fv2* susceptibility gene, (B6 x A.BY)F_1 mice are more susceptible to FV infection and develop splenomegaly (10). Cells from both bone marrow (Fig. 4A) and spleen (data not shown) were analyzed at 7 dpi. No significant perturbations in the proportions of erythroid cells, B-cells, T-cells and myeloid cells were observed in either tissue (Fig. 4B and data not shown). However, higher levels of viral infection were observed in each of these cell subsets in (B6 *Apobec3*$^{-/-}$ x A.BY)F_1 versus (B6 *Apobec3*$^{+/+}$ x A.BY)F_1 mice (Fig. 4C and Table I).

Less efficient induction of germinal center B cells in Apobec3-deficient mice

Direct viral infection of various cell subsets could result in altered adaptive immune response leading in turn to a lack of antibody affinity maturation. We next investigated potential alterations in B cell subpopulations in (B6 *Apobec3*$^{-/-}$ x A.BY)F_1 versus (B6 *Apobec3*$^{+/+}$ x A.BY)F_1 mice at 7 dpi. Antigen-specific B cell development initiates in the bone marrow where initial immunoglobulin gene rearrangements and maturation occurs. IgM and IgD can be used as markers of B cell maturation, while syndecan-1 (CD138) can be used to mark B cells that have become antibody-secreting cells (Fig. 5A). FV infection resulted in a significant (~30%) decrease in the proportion of B cells in the bone marrow of both (B6 *Apobec3*$^{+/+}$ x A.BY)F_1 and (B6 *Apobec3*$^{-/-}$ x A.BY)F_1 mice (Fig. 5B, *upper left* panel). Similar phenomena were also observed for both IgM^+ and IgD^+ B cells at 7 dpi (Fig. 5B, *upper right* and *lower left* panels). Thus, we found no obvious defects in early B cell proportions associated with B6 Apobec3 deficiency at 7 dpi. Interestingly, there was a significant increase in $CD138^+$ plasmablasts that had migrated to the bone marrow of FV-infected (B6 *Apobec3*$^{+/+}$ x A.BY)F_1, but not (B6 *Apobec3*$^{-/-}$ x A.BY)F_1 mice at 7 dpi (Fig. 5B, *lower right* panel). This result suggested possible differences in B-cell subpopulations in secondary lymphoid organs.

Upon encountering antigen, B cells proliferate in secondary lymphoid organs and undergo affinity maturation in structures known as germinal centers (GC) (27). Subsequently, selected antigen-specific B cells develop into $CD138^+$ plasmablasts that migrate back to the bone marrow to become antibody-secreting plasma cells (40). Following the detection of higher levels of $CD138^+$ plasmablasts in the bone marrow of FV-infected (B6 *Apobec3*$^{+/+}$ x A.BY)F_1 mice, we sought to quantify the frequencies of GC B cells and plasmablasts in the

spleen (Fig. 6A). GC B cells can be preferentially marked with peanut agglutinin (PNA), which reacts with O-linked glycans, or GL7, which correspond to α2,6-linked sialic acid present on lactosamine chains (41). High levels of foreign antigens associated with virus infection are thought to drive germinal center formation and antigen-specific B cell development. Consistent with this notion, acute FV infection of (B6 *Apobec3*$^{+/+}$ x A.BY)F_1 mice resulted in a 2.0- and 2.3-fold increase in the proportion of splenic GC B cells ($GL7^+$) and $CD138^+$ plasmablasts, respectively, relative to uninfected (B6 *Apobec3*$^{+/+}$ x A.BY)F_1 mice (Fig. 6B). Of note, (B6 *Apobec3*$^{-/-}$ x A.BY)F_1 strains exhibited significantly lower levels of induction of these cell subpopulations (Fig. 7B), despite the fact that these mice strains display higher levels of viremia (Table I). In a separate cohort of mice, we detected higher frequencies of PNA^{hi} GC B cells in infected (B6 *Apobec3*$^{+/+}$ x A.BY)F_1 mice compared to infected (B6 *Apobec3*$^{-/-}$ x A.BY)F_1 mice (not shown). Thus, the presence of B6 Apobec3 is associated with greater induction of germinal center B cell and plasmablast cell subpopulations in the spleen during acute FV infection.

Apobec3 influences immunoglobulin levels during acute FV infection

Suppressed induction of germinal center B cells and plasmablasts during acute FV infection of B6 Apobec3-deficient mice despite higher viral antigen loads suggested that B-cell function in these mice was either blocked or dysregulated. To investigate potential humoral immune dysregulation, we assessed whether FV-infected B6 Apobec3-deficient mice exhibited hypergammaglobulinemia, a hallmark of aberrant polyclonal B cell activation (42,43).

Our results revealed that uninfected B6 *Apobec3*$^{+/+}$ and B6 *Apobec3*$^{-/-}$ mice display similar levels of total IgM and IgG in the plasma (Fig. 7A). However, at one week following FV infection, both total IgM (Fig. 7A, *left* panel) and IgG levels (Fig. 7A, *right* panel) were significantly higher in Apobec3-deficient mice compared to wild-type. To investigate whether any IgG subclasses were preferentially induced in FV infected Apobec3-deficient mice, we measured plasma titers for IgG2b, IgG3 and IgG1 (we confirmed that these B6 mice lack detectable levels of IgG2a (44)). The titers of these IgG subclasses did not vary significantly between uninfected wild-type and Apobec3-deficient mice. However, upon FV infection, there was a statistically significant increase in IgG2b and IgG3 titers in the Apobec3-deficient compared to the wild-type mice (Fig. 7B). There was also a trend for increased IgG1 and IgA expression in Apobec3-deficient mice (Fig. 7B). However, by 28 dpi, the total IgG titers in wild-type mice increased to the same elevated levels as Apobec3-deficient mice (not shown). These findings revealed that Apobec3 activity delayed the onset of hypergammaglobulinemia during FV infection.

DISCUSSION

The recent identification of Apobec3 as *Rfv3* (10), a gene that influences neutralizing antibody responses against Friend retrovirus infection, immediately raised the issue of how the innate Apobec3 enzyme achieves this effect on the humoral immune response. Our studies indicate that Apobec3 does not act directly in B cells by promoting somatic hypermutation and antibody affinity maturation like the AID cytidine deaminase. Rather, Apobec3 appears to act in a more indirect manner by protecting key immune cells needed for optimal neutralizing antibody responses during FV infection. These results strengthen an emerging concept that the early host response occurring during pathogenic virus infection can have a profound impact on disease recovery. This could be due to the ability of innate immune responses to dampen early pathological events that may otherwise compromise the integrity and efficacy of subsequent adaptive immune responses. This concept may be particularly relevant for viruses that directly infect immune cells of the host, which, in the case of FV infection, were protected by Apobec3.

Our findings demonstrate that the presence of the B6 Apobec3 gene promotes more vigorous induction or development of germinal center B cells and plasmablasts that participate in the production of high-affinity antibodies. In addition, Apobec3 delays the onset of hypergammaglobulinemia, a hallmark of aberrant B-cell activation (42,43). Together, these findings suggest that Apobec3 preserves B cell function during acute FV infection and facilitates antibody affinity maturation. These results provide a working model (Fig. 8) to further dissect the sequence of events that underlie the weaker neutralizing antibody response occurring in mice with defective Apobec3 function.

Notably, B6 Apobec3-deficient mice at 7 dpi exhibited lower levels of splenic GC B cells but higher levels of total immunoglobulins in plasma. We previously reported that at 14 dpi, FV-infected B6 Apobec3-deficient mice had lower levels of FV-specific IgG antibodies compared to mice encoding B6 Apobec3 (10). Thus, the induced immunoglobulins in B6 Apobec3-deficient mice are likely not virus-specific, and likely developed in an extrafollicular manner (45). While it is known that CD4+ T cells (42), viral proteins (46) and the LDV component of the original FV stock (47) can directly participate in hypergammaglobulinemia induction, the impact of Apobec3 on these parameters requires further study. Finally, it remains unknown whether the *Rfv3* phenotype is solely due to the ability of Apobec3 to protect B-cells from FV infection, or whether protection of other cells types also plays a role. Uncontrolled FV replication in erythroblasts, myeloid cells and T-cells could result in displacement of other cell types and/or the aberrant release of cytokines that could misdirect the B-cell response. FV infection of dendritic cells (48) and follicular $CD4^+$ T cells (49), in particular, may have a dramatic impact on subsequent antibody responses. Dissecting the contribution of individual cell types in the Apobec3-mediated influence on humoral immunity will require adoptive transfer studies or FV infection of transgenic mice where Apobec3 is preferentially expressed only in specific immune cell subpopulations.

Our results suggest that decreased B-cell pathology during acute infection contributes to the ability of Apobec3 to promote an effective FV-specific neutralizing antibody response (the hallmark of the *Rfv3* phenotype). While this would suggest that antiviral interventions during the acute phase of FV infection may also strengthen antibody responses, we hypothesize that the unique biology of Apobec3 may particularly promote this process. Apobec3 activity results in the release of noninfectious particles that present the envelope glycoprotein, the major target of neutralizing antibodies in FV infection (34,50), as functional, fusion-competent trimers. Thus, in contrast to other innate intervention mechanisms, Apobec3 activity not only could reduce FV-induced pathology, but it may also present viral envelope antigens in a manner that is highly suitable to elicit an effective antibody response. The possibility that $Apobec3^+$ viral particles serve as “endogenous vaccines” in the FV model system is currently being explored. Notably, presenting functional envelope trimers for eliciting neutralizing antibody responses has been used to justify the development of HIV-1 vaccines based on noninfectious Virus-Like Particles (VLPs) (51,52).

The nature of a protective neutralizing antibody response against pathogenic retroviruses remains unclear. High-affinity envelope-specific antibodies, high levels of low-affinity virus-specific antibodies that confer high avidity binding, antibodies that bind to epitopes critical for envelope-mediated fusion and specific IgG subclasses that mediate potent antibody-dependent cellular cytotoxicity could all be important features of a potent neutralizing antibody response. The results of our hapten immunization studies may offer additional clues. One month following FV infection/hapten boosting, the total NP-specific binding titers were similar between wild-type and Apobec3-deficient mice, but the binding affinities were significantly lower for mice lacking Apobec3 (Fig. 3). Of note, we previously

found that total virus-specific binding antibodies at 28 dpi were not significantly different between mice with or without the B6 Apobec3 gene, but neutralizing antibody responses were significantly higher in B6 Apobec3$^+$ mice [(10) and our unpublished results]. We hypothesize that a potent virus-specific neutralizing antibody response includes a significant proportion of virus-specific antibodies that exhibit high affinity to the envelope glycoprotein (Fig. 8). Thus, a potent virus-specific neutralizing antibody response may be dictated as much by the quality as the quantity of virus-specific antibodies. Profiling the FV-specific antibody repertoire in infected B6 Apobec3$^+$ and B6 Apobec3-deficient mice may help dissect the molecular characteristics of a protective versus a non-protective antibody response against this pathogenic retrovirus infection.

The importance of Apobec3 in human retrovirus infections has been highlighted by the identification of specific viral mechanisms that subvert this response. HIV-1 encodes a protein known as Vif that specifically antagonizes two human Apobec3 homologues, Apobec3G and Apobec3F (53,54). Vif binds to Apobec3G and Apobec3F and links these deaminases to components of an E3-ubiquitin ligase complex that promotes polyubiquitylation and subsequent proteasome-mediated degradation of these enzymes (53,55–58). Thus, the function of two critical human Apobec3 proteins in HIV-1 infected individuals is impaired, analogous to *Rfv3* susceptible mouse strains. Notably, HIV-1 infected individuals rarely mount a strong HIV-1 specific neutralizing antibody response. While the heterogeneity and structural features of the HIV-1 envelope glycoprotein are considered the primary evasive mechanisms, extensive humoral immune dysfunction, such as hypergammaglobulinemia and aberrant polyclonal B cell activation (59), loss in memory B cell subsets (60) and germinal center destruction in the gastrointestinal tract (61), during acute HIV-1 infection is gaining attention as a contributing force for poor neutralizing antibody responses. B-cell defects also appear to underlie the poor virus- and hapten-specific antibody responses occurring in FV-infected mice lacking Apobec3 (Fig. 8).

By analogy, our studies raise the possibility that augmenting Apobec3G/Apobec3F function during acute HIV-1 infection may help strengthen the neutralizing antibody response by dampening virus-induced pathology, while facilitating the release of noninfectious particles. This possibility may be experimentally tested in pathogenic SIV infection models in rhesus macaques, where recently, mutations in SIV Vif that compromise its interplay with the E3 ligase component Elongin C resulted in the rescue of CD4$^+$ T cells and virus-specific antibody responses (62). If true, manipulating Apobec3 activity to improve HIV-1 specific neutralizing antibody responses could significantly impact future HIV-1 vaccine development strategies.

Note added post review

Following the submission of this manuscript, a study performed by Tsuji-Kawahara *et al* was published online (63). This study confirmed our initial findings that Apobec3 influences the Friend retrovirus-specific neutralizing antibody response (10), the distinguishing hallmark of *Rfv3* (6,33). Complementing the results we present here, Tsuji-Kawahara *et al.* also provided evidence favoring an indirect mechanism for how Apobec3 influences neutralizing antibody responses by demonstrating: (1) no difference in antibody binding titers following immunization with DNP-Ficoll and DNP-OVA in uninfected mice with or without the B6 Apobec3 gene; (2) increased FV infection of spleen Ter119+ and B cells in the absence of B6 Apobec3; and (3) increased B-cell activation and defects in B-cell maturation in the spleen of B6 Apobec3-deficient mice at 10 dpi. However, unlike the data we present here, Tsuji-Kawahara *et al* did not present evidence that the B6 Apobec3 gene promotes antibody affinity maturation, germinal center B cell induction and plasmablast development during acute infection (7 dpi) by protecting multiple Apobec3+ cellular subsets in *both* the bone marrow and spleen from FV infection. Finally, Tsuji-Kawarahara *et al.*

suggested that a recessive BAFF-R deficiency in the A/WySn strain contributes more to the *Rfv3* phenotype than Apobec3. This conclusion is based on the authors' comparison of 28 dpi viremia for (B6 x A/WySn)F_1 and (B6.Apobec3$^{-/-}$ x A/WySn)F_1 mice. Surprisingly, no data was presented for congenic (B6 BAFF-R$^{-/-}$ x A/WySn)F_1 mice, making it currently impossible to ascertain the relative contributions of BAFF-R and Apobec3 in the recovery of (B6 x A/WySn)F_1 mice. Importantly, in our study, all the strains utilized [B6, (B6 x A.BY)F_1 and (B6 x BALB/c)F_1] express the dominant wild-type BAFF-R gene from the B6 background. Thus, BAFF-R deficiency does not impact any of our presented results.

Acknowledgments

We would like to thank Richard Locksley (UCSF) for advice on the hapten immunization studies, and Roberta Pelanda and Raul Torres (UCD) for discussion.

References

1. Hasenkrug KJ, Dittmer U. Immune control and prevention of chronic Friend retrovirus infection. Front Biosci 2007;12:1544–1551. [PubMed: 17127401]
2. Miyazawa M, Tsuji-Kawahara S, Kanari Y. Host genetic factors that control immune responses to retrovirus infections. Vaccine 2008;26:2981–2996. [PubMed: 18255203]
3. Lilly F. Fv-2: identification and location of a second gene governing the spleen focus response to Friend leukemia virus in mice. Journal of the National Cancer Institute 1970;45:163–169. [PubMed: 5449211]
4. Persons DA, Paulson RF, Loyd MR, Herley MT, Bodner SM, Bernstein A, Correll PH, Ney PA. Fv2 encodes a truncated form of the Stk receptor tyrosine kinase. Nat Genet 1999;23:159–165. [PubMed: 10508511]
5. Chesebro B, Wehrly K. Studies on the role of the host immune response in recovery from Friend virus leukemia. II. Cell-mediated immunity. The Journal of experimental medicine 1976;143:85–99. [PubMed: 1081583]
6. Chesebro B, Wehrly K. Identification of a non-H-2 gene (Rfv-3) influencing recovery from viremia and leukemia induced by Friend virus complex. Proceedings of the National Academy of Sciences of the United States of America 1979;76:425–429. [PubMed: 284359]
7. Hasenkrug KJ, Valenzuela A, Letts VA, Nishio J, Chesebro B, Frankel WN. Chromosome mapping of Rfv3, a host resistance gene to Friend murine retrovirus. Journal of virology 1995;69:2617–2620. [PubMed: 7884913]
8. Super HJ, Hasenkrug KJ, Simmons S, Brooks DM, Konzek R, Sarge KD, Morimoto RI, Jenkins NA, Gilbert DJ, Copeland NG, Frankel W, Chesebro B. Fine mapping of the friend retrovirus resistance gene, Rfv3, on mouse chromosome 15. Journal of virology 1999;73:7848–7852. [PubMed: 10438878]
9. Kanari Y, Clerici M, Abe H, Kawabata H, Trabattoni D, Caputo SL, Mazzotta F, Fujisawa H, Niwa A, Ishihara C, Takei YA, Miyazawa M. Genotypes at chromosome 22q12-13 are associated with HIV-1-exposed but uninfected status in Italians. AIDS (London, England) 2005;19:1015–1024.
10. Santiago ML, Montano M, Benitez R, Messer RJ, Yonemoto W, Chesebro B, Hasenkrug KJ, Greene WC. Apobec3 encodes Rfv3, a gene influencing neutralizing antibody control of retrovirus infection. Science (New York, NY) 2008;321:1343–1346.
11. Santiago, ML.; Greene, WC. The role of the Apobec3 family of cytidine deaminases in innate immunity, G-to-A hypermutation and evolution of retroviruses. In: Domingo, E.; Parrish, CR.; Holland, JJ., editors. Origin and Evolution of Viruses. Academic Press; London, UK: 2008. p. 183-206.
12. Bishop KN, Verma M, Kim EY, Wolinsky SM, Malim MH. APOBEC3G inhibits elongation of HIV-1 reverse transcripts. PLoS pathogens 2008;4:e1000231. [PubMed: 19057663]
13. Soros VB, Yonemoto W, Greene WC. Newly Synthesized APOBEC3G Is Incorporated into HIV Virions, Inhibited by HIV RNA, and Subsequently Activated by RNase H. PLoS pathogens 2007;3:e15. [PubMed: 17291161]

14. Harris RS, Bishop KN, Sheehy AM, Craig HM, Petersen-Mahrt SK, Watt IN, Neuberger MS, Malim MH. DNA deamination mediates innate immunity to retroviral infection. Cell 2003;113:803–809. [PubMed: 12809610]
15. Lecossier D, Bouchonnet F, Clavel F, Hance AJ. Hypermutation of HIV-1 DNA in the absence of the Vif protein. Science (New York, NY) 2003;300:1112.
16. Mangeat B, Turelli P, Caron G, Friedli M, Perrin L, Trono D. Broad antiretroviral defence by human APOBEC3G through lethal editing of nascent reverse transcripts. Nature 2003;424:99–103. [PubMed: 12808466]
17. Zhang H, Yang B, Pomerantz RJ, Zhang C, Arunachalam SC, Gao L. The cytidine deaminase CEM15 induces hypermutation in newly synthesized HIV-1 DNA. Nature 2003;424:94–98. [PubMed: 12808465]
18. Mbisa JL, Barr R, Thomas JA, Vandegraaff N, Dorweiler IJ, Svarovskaia ES, Brown WL, Mansky LM, Gorelick RJ, Harris RS, Engelman A, Pathak VK. HIV-1 cDNAs Produced in the Presence of APOBEC3G Exhibit Defects in Plus-Strand DNA Transfer and Integration. Journal of virology. 2007
19. Luo K, Wang T, Liu B, Tian C, Xiao Z, Kappes J, Yu XF. Cytidine deaminases APOBEC3G and APOBEC3F interact with human immunodeficiency virus type 1 integrase and inhibit proviral DNA formation. Journal of virology 2007;81:7238–7248. [PubMed: 17428847]
20. Okeoma CM, Petersen J, Ross SR. Expression of murine APOBEC3 alleles in different mouse strains and their effect on mouse mammary tumor virus infection. Journal of virology 2009;83:3029–3038. [PubMed: 19153233]
21. Takeda E, Tsuji-Kawahara S, Sakamoto M, Langlois MA, Neuberger MS, Rada C, Miyazawa M. Mouse APOBEC3 restricts friend leukemia virus infection and pathogenesis in vivo. Journal of virology 2008;82:10998–11008. [PubMed: 18786991]
22. Abudu A, Takaori-Kondo A, Izumi T, Shirakawa K, Kobayashi M, Sasada A, Fukunaga K, Uchiyama T. Murine retrovirus escapes from murine APOBEC3 via two distinct novel mechanisms. Curr Biol 2006;16:1565–1570. [PubMed: 16890533]
23. Conticello SG, Thomas CJ, Petersen-Mahrt SK, Neuberger MS. Evolution of the AID/APOBEC family of polynucleotide (deoxy)cytidine deaminases. Molecular biology and evolution 2005;22:367–377. [PubMed: 15496550]
24. Muramatsu M, Kinoshita K, Fagarasan S, Yamada S, Shinkai Y, Honjo T. Class switch recombination and hypermutation require activation-induced cytidine deaminase (AID), a potential RNA editing enzyme. Cell 2000;102:553–563. [PubMed: 11007474]
25. Low A, Okeoma CM, Lovsin N, de las Heras M, Taylor TH, Peterlin BM, Ross SR, Fan H. Enhanced replication and pathogenesis of Moloney murine leukemia virus in mice defective in the murine APOBEC3 gene. Virology 2009;385:455–463. [PubMed: 19150103]
26. Okeoma CM, Lovsin N, Peterlin BM, Ross SR. APOBEC3 inhibits mouse mammary tumour virus replication in vivo. Nature 2007;445:927–930. [PubMed: 17259974]
27. Jacob J, Kelsoe G, Rajewsky K, Weiss U. Intraclonal generation of antibody mutants in germinal centres. Nature 1991;354:389–392. [PubMed: 1956400]
28. Smith KG, Weiss U, Rajewsky K, Nossal GJ, Tarlinton DM. Bcl-2 increases memory B cell recruitment but does not perturb selection in germinal centers. Immunity 1994;1:803–813. [PubMed: 7895168]
29. Matsumoto M, Lo SF, Carruthers CJ, Min J, Mariathasan S, Huang G, Plas DR, Martin SM, Geha RS, Nahm MH, Chaplin DD. Affinity maturation without germinal centres in lymphotoxin-alpha-deficient mice. Nature 1996;382:462–466. [PubMed: 8684487]
30. Herzenberg LA, Black SJ, Tokuhisa T, Herzenberg LA. Memory B cells at successive stages of differentiation. Affinity maturation and the role of IgD receptors. The Journal of experimental medicine 1980;151:1071–1087. [PubMed: 6966317]
31. Furukawa K, Akasako-Furukawa A, Shirai H, Nakamura H, Azuma T. Junctional amino acids determine the maturation pathway of an antibody. Immunity 1999;11:329–338. [PubMed: 10514011]
32. Shimizu T, Oda M, Azuma T. Estimation of the relative affinity of B cell receptor by flow cytometry. Journal of immunological methods 2003;276:33–44. [PubMed: 12738357]

33. Doig D, Chesebro B. Anti-Friend virus antibody is associated with recovery from viremia and loss of viral leukemia cell-surface antigens in leukemic mice. Identification of Rfv-3 as a gene locus influencing antibody production. The Journal of experimental medicine 1979;150:10–19. [PubMed: 286744]
34. Britt WJ, Chesebro B. Use of monoclonal anti-gp70 antibodies to mimic the effects of the Rfv-3 gene in mice with Friend virus-induced leukemia. J Immunol 1983;130:2363–2367. [PubMed: 6833759]
35. Robertson SJ, Ammann CG, Messer RJ, Carmody AB, Myers L, Dittmer U, Nair S, Gerlach N, Evans LH, Cafruny WA, Hasenkrug KJ. Suppression of acute anti-friend virus CD8+ T-cell responses by coinfection with lactate dehydrogenase-elevating virus. Journal of virology 2008;82:408–418. [PubMed: 17959678]
36. Marques R, Antunes I, Eksmond U, Stoye J, Hasenkrug K, Kassiotis G. B lymphocyte activation by coinfection prevents immune control of friend virus infection. J Immunol 2008;181:3432–3440. [PubMed: 18714015]
37. Chesebro B, Britt W, Evans L, Wehrly K, Nishio J, Cloyd M. Characterization of monoclonal antibodies reactive with murine leukemia viruses: use in analysis of strains of friend MCF and Friend ecotropic murine leukemia virus. Virology 1983;127:134–148. [PubMed: 6305011]
38. Mikl MC I, Watt N, Lu M, Reik W, Davies SL, Neuberger MS, Rada C. Mice deficient in APOBEC2 and APOBEC3. Molecular and cellular biology 2005;25:7270–7277. [PubMed: 16055735]
39. Dittmer U, Race B, Peterson KE, Stromnes IM, Messer RJ, Hasenkrug KJ. Essential roles for CD8+ T cells and gamma interferon in protection of mice against retrovirus-induced immunosuppression. Journal of virology 2002;76:450–454. [PubMed: 11739713]
40. Takahashi Y, Dutta PR, Cerasoli DM, Kelsoe G. In situ studies of the primary immune response to (4-hydroxy-3-nitrophenyl)acetyl. V. Affinity maturation develops in two stages of clonal selection. The Journal of experimental medicine 1998;187:885–895. [PubMed: 9500791]
41. Naito Y, Takematsu H, Koyama S, Miyake S, Yamamoto H, Fujinawa R, Sugai M, Okuno Y, Tsujimoto G, Yamaji T, Hashimoto Y, Itohara S, Kawasaki T, Suzuki A, Kozutsumi Y. Germinal center marker GL7 probes activation-dependent repression of N-glycolylneuraminic acid, a sialic acid species involved in the negative modulation of B-cell activation. Molecular and cellular biology 2007;27:3008–3022. [PubMed: 17296732]
42. Hunziker L, Recher M, Macpherson AJ, Ciurea A, Freigang S, Hengartner H, Zinkernagel RM. Hypergammaglobulinemia and autoantibody induction mechanisms in viral infections. Nature immunology 2003;4:343–349. [PubMed: 12627229]
43. Klinman DM, Morse HC 3rd. Characteristics of B cell proliferation and activation in murine AIDS. J Immunol 1989;142:1144–1149. [PubMed: 2464640]
44. Morgado MG, Cam P, Gris-Liebe C, Cazenave PA, Jouvin-Marche E. Further evidence that BALB/c and C57BL/6 gamma 2a genes originate from two distinct isotypes. The EMBO journal 1989;8:3245–3251. [PubMed: 2510996]
45. MacLennan IC, Toellner KM, Cunningham AF, Serre K, Sze DM, Zuniga E, Cook MC, Vinuesa CG. Extrafollicular antibody responses. Immunological reviews 2003;194:8–18. [PubMed: 12846803]
46. Montes CL, Acosta-Rodriguez EV, Merino MC, Bermejo DA, Gruppi A. Polyclonal B cell activation in infections: infectious agents' devilry or defense mechanism of the host? Journal of leukocyte biology 2007;82:1027–1032. [PubMed: 17615380]
47. Coutelier JP, Coulie PG, Wauters P, Heremans H, van der Logt JT. In vivo polyclonal B-lymphocyte activation elicited by murine viruses. Journal of virology 1990;64:5383–5388. [PubMed: 1976818]
48. Balkow S, Krux F, Loser K, Becker JU, Grabbe S, Dittmer U. Friend retrovirus infection of myeloid dendritic cells impairs maturation, prolongs contact to naive T cells, and favors expansion of regulatory T cells. Blood 2007;110:3949–3958. [PubMed: 17699743]
49. King C, Tangye SG, Mackay CR. T follicular helper (TFH) cells in normal and dysregulated immune responses. Annual review of immunology 2008;26:741–766.

50. Hasenkrug KJ, Brooks DM, Robertson MN, Srinivas RV, Chesebro B. Immunoprotective determinants in friend murine leukemia virus envelope protein. Virology 1998;248:66–73. [PubMed: 9705256]
51. Crooks ET, Moore PL, Franti M, Cayanan CS, Zhu P, Jiang P, de Vries RP, Wiley C, Zharkikh I, Schulke N, Roux KH, Montefiori DC, Burton DR, Binley JM. A comparative immunogenicity study of HIV-1 virus-like particles bearing various forms of envelope proteins, particles bearing no envelope and soluble monomeric gp120. Virology 2007;366:245–262. [PubMed: 17580087]
52. Hammonds J, Chen X, Zhang X, Lee F, Spearman P. Advances in methods for the production, purification, and characterization of HIV-1 Gag-Env pseudovirion vaccines. Vaccine 2007;25:8036–8048. [PubMed: 17936444]
53. Sheehy AM, Gaddis NC, Malim MH. The antiretroviral enzyme APOBEC3G is degraded by the proteasome in response to HIV-1 Vif. Nature medicine 2003;9:1404–1407.
54. Zheng YH, Irwin D, Kurosu T, Tokunaga K, Sata T, Peterlin BM. Human APOBEC3F is another host factor that blocks human immunodeficiency virus type 1 replication. Journal of virology 2004;78:6073–6076. [PubMed: 15141007]
55. Stopak K, de Noronha C, Yonemoto W, Greene WC. HIV-1 Vif blocks the antiviral activity of APOBEC3G by impairing both its translation and intracellular stability. Mol Cell 2003;12:591–601. [PubMed: 14527406]
56. Marin M, Rose KM, Kozak SL, Kabat D. HIV-1 Vif protein binds the editing enzyme APOBEC3G and induces its degradation. Nature medicine 2003;9:1398–1403.
57. Conticello SG, Harris RS, Neuberger MS. The Vif protein of HIV triggers degradation of the human antiretroviral DNA deaminase APOBEC3G. Curr Biol 2003;13:2009–2013. [PubMed: 14614829]
58. Mehle A, Strack B, Ancuta P, Zhang C, McPike M, Gabuzda D. Vif overcomes the innate antiviral activity of APOBEC3G by promoting its degradation in the ubiquitin-proteasome pathway. J Biol Chem 2004;279:7792–7798. [PubMed: 14672928]
59. Lane HC, Masur H, Edgar LC, Whalen G, Rook AH, Fauci AS. Abnormalities of B-cell activation and immunoregulation in patients with the acquired immunodeficiency syndrome. N Engl J Med 1983;309:453–458. [PubMed: 6224088]
60. Moir S, Fauci AS. Pathogenic mechanisms of B-lymphocyte dysfunction in HIV disease. J Allergy Clin Immunol 2008;122:12–19. quiz 20–11. [PubMed: 18547629]
61. Levesque MC, Moody MA, Hwang KK, Marshall DJ, Whitesides JF, Amos JD, Gurley TC, Allgood S, Haynes BB, Vandergrift NA, Plonk S, Parker DC, Cohen MS, Tomaras GD, Goepfert PA, Shaw GM, Schmitz JE, Eron JJ, Shaheen NJ, Hicks CB, Liao HX, Markowitz M, Kelsoe G, Margolis DM, Haynes BF. Polyclonal B cell differentiation and loss of gastrointestinal tract germinal centers in the earliest stages of HIV-1 infection. PLoS medicine 2009;6:e1000107. [PubMed: 19582166]
62. Schmitt K, Hill MS, Ruiz A, Culley N, Pinson DM, Wong SW, Stephens EB. Mutations in the highly conserved SLQYLA motif of Vif in a simian-human immunodeficiency virus result in a less pathogenic virus and are associated with G-to-A mutations in the viral genome. Virology 2009;383:362–372. [PubMed: 19027134]
63. Tsuji-Kawahara S, Chikaishi T, Takeda E, Kato M, Kinoshita S, Kajiwara E, Takamura S, Miyazawa M. Persistence of viremia and production of neutralizing antibodies differentially regulated by polymorphic APOBEC3 and BAFF-R loci in Friend virus-infected mice. Journal of virology.

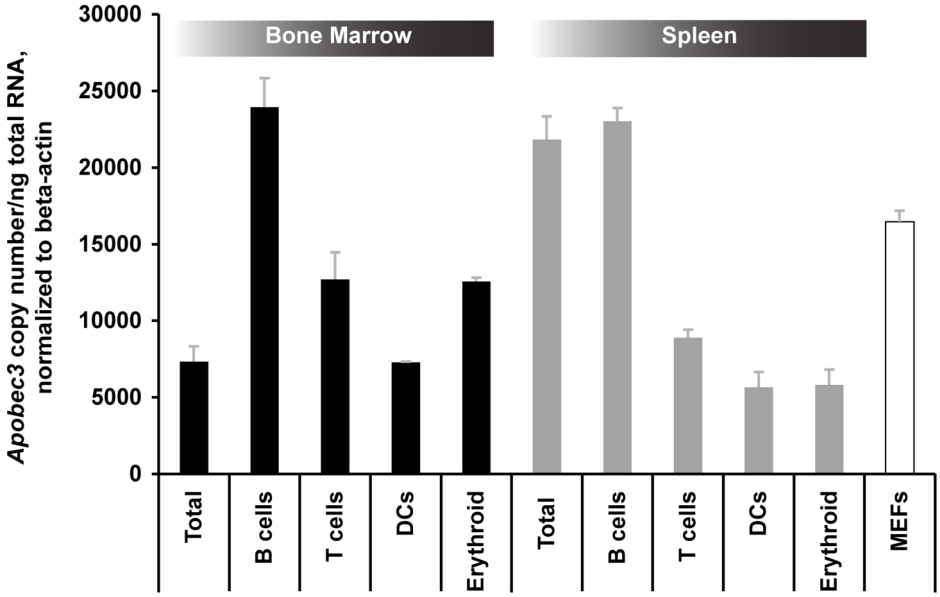

Figure 1.

Expression of *Apobec3* mRNA in bone marrow and spleen cell subpopulations. B-cells ($CD19^+$), T-cells ($CD90.2^+$), erythroid ($Ter119^+$) and dendritic cells ($CD11c^+$) were magnetically purified from bone marrow or spleen in B6 mice and subjected to quantitative RT-PCR. Mouse embryonic fibroblasts (MEFs) were derived from B6 mice. Note that all of these cell subpopulations express readily detectable *Apobec3* mRNA, with the highest levels of expression found in B cells.

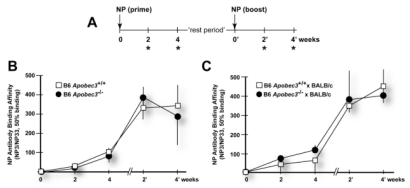

Figure 2.

Apobec3 does not influence NP-specific IgG1 affinity maturation. (A) Immunization schedule. Mice were primed and boosted with 100 μg NP_{26}-CGG and plasma samples collected at 2 and 4 weeks after priming and boosting (*). Timepoints from the time of the NP-boost were designated as weeks 0′, 2′ and 4′. The "rest period" corresponds to the time interval between the bleed 4 weeks after NP-priming and the timepoint of NP-boosting. (B) Kinetics of NP-specific antibody affinity maturation in B6 mice. Plasma samples from B6 *Apobec3*$^{+/+}$ (n=7) and *Apobec3*$^{-/-}$ mice (n=7) were subjected to a differential NP-binding ELISA. The relative binding affinity of NP-specific antibodies was expressed as the ratio of the mean 50% binding titers to low (NP_3)- versus high (NP_{33})-molar hapten reactivities multiplied by 100. Standard deviations were indicated as vertical lines. The rest period for this cohort was 2 weeks. (C) Kinetics of affinity maturation in (B6 x BALB/c)F_1mice. Plasma samples from (B6 *Apobec3*$^{+/+}$ x BALB/c) F_1 (n=7) and (B6 *Apobec3*$^{-/-}$ x BALB/c) F_1 (n=7) were subjected to a differential NP-ELISA and relative binding affinities are shown. The rest period for this cohort was 2 weeks.

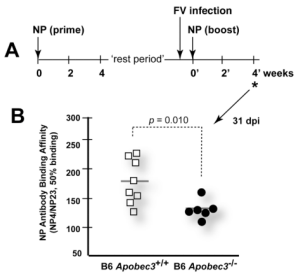

Figure 3.

Apobec3 promotes NP-specific antibody affinity maturation in the context of FV infection. (A) FV infection prior to NP boosting. Three days prior to boosting with 100μg NP_{26}-CGG, the primed mice were infected with 7500 SFFU of FV. The relative binding affinity of NP-specific antibodies were measured 4 weeks (*) following the NP-boost. This timepoint corresponds to 31 days post-infection (dpi). The rest period corresponds to the time interval between the bleed 4 weeks after NP-priming and the timepoint of NP-boosting, and corresponds to 16 weeks for this cohort. (B) Antibody affinity was estimated using a differential NP ELISA. NP-specific antibodies from B6 *Apobec3*$^{-/-}$ mice showed significantly lower binding affinity compared to wild-type mice. *p* values were calculated using a 2-tailed Student's *t* test.

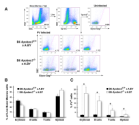

Figure 4.

B6 Apobec3 protects specific subpopulations of bone marrow cells from acute FV infection. (A) Gating strategy for assessing FV infection. Live bone marrow cells were gated based on forward and side scatter, and the percentage of specific cell subpopulations (in this case $Ter119^+$erythroblasts) was assessed within this live cell population. A Glyco-gag-specific monoclonal antibody (MAb 34), coupled with APC-conjugated secondary antibody, was used to detect FV-infected cells. Uninfected cells had <1% reactivity with MAb34. Using these gates, the percentages of FV^+ cells were estimated. Representative panels from B6 *Apobec3*$^+$ and deficient F_1 mice are highlighted. (B) Bone marrow cell subpopulations in FV infected mice. The proportion of erythroid ($Ter119^+$), B ($CD19^+$), T ($CD3^+$) and myeloid ($CD11b^+$) cells in live bone marrow cells were quantified. There was no significant difference in the proportion of these cell subpopulations found in B6 *Apobec3*$^+$ (n=8) and B6 *Apobec3*-deficient (n=8) F_1 mice. Error bars depict standard error of the mean. (C) Higher levels of FV-infected cells in multiple bone marrow subpopulations were detected in mice lacking B6 Apobec3. FV^+ erythroid, B, T and myeloid cells were quantified by flow cytometry. Statistical analyses were performed using a 2-tailed Student's *t*-test: *, $p<0.05$. The data corresponds to Cohort 2 as outlined in Table I.

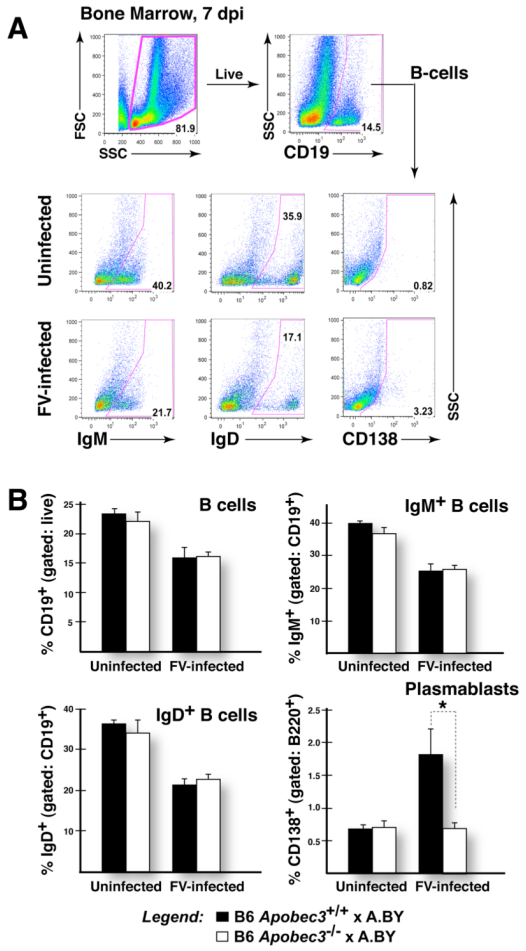

Figure 5.

Bone marrow B-cell perturbations in FV-infected B6 *Apobec3*$^{+}$ and B6 *Apobec3*-deficient F_1 mice. (A) Gating strategy. B-cells (CD19^{+} or B220^{+}) present within the live cell gate were analyzed for the proportion of IgM^{+}, IgD^{+} and CD138^{+}. (B) B-cell subpopulations in infected versus uninfected mice. The mean percentages were plotted, with vertical lines depicting the standard error of the mean. The samples sizes were: (B6 *Apobec3*$^{+/+}$ x A.BY) F_1 (uninfected, n=7; infected, n=8); (B6 *Apobec3*$^{-/-}$ x A.BY) F_1 (uninfected, n=7; infected, n=8). Data were subjected to a 2-tailed Student's *t*-test. *, $p<0.05$. FV infection resulted in a decline in total, IgM^{+} and IgD^{+} B cells. In contrast, CD138^{+} B cells (plasmablasts) were preferentially induced in FV-infected B6 *Apobec3*$^{+}$ F_1 mice.

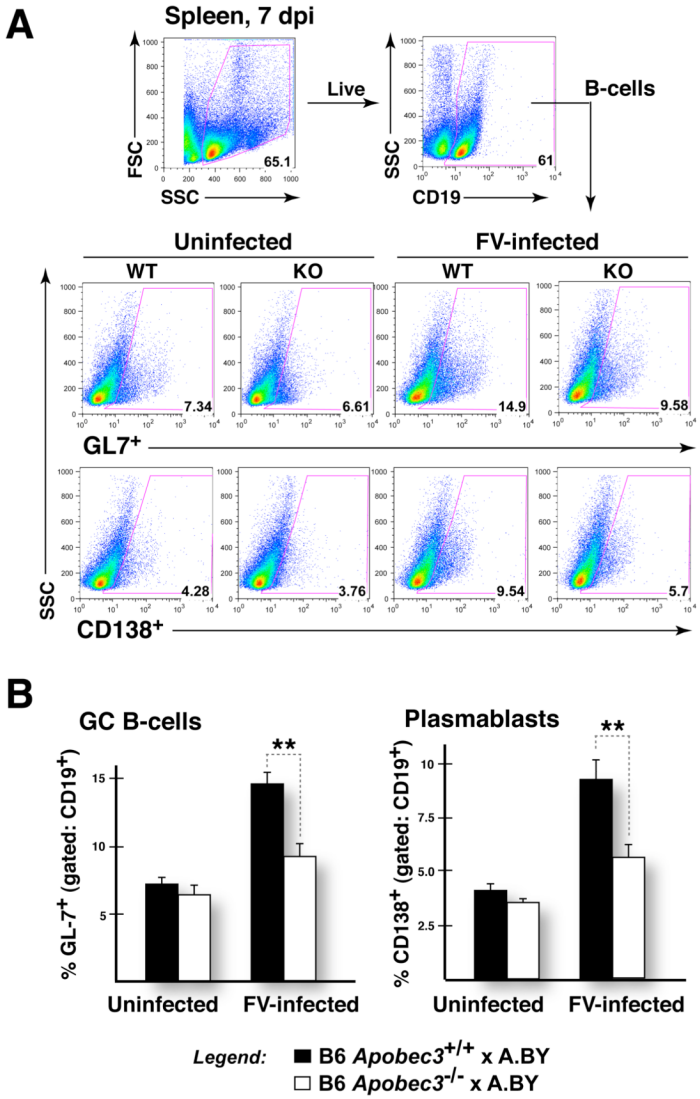

Figure 6.

Suppressed induction of splenic germinal center B cells and plasmablasts in FV-infected B6 Apobec3-deficient F_1 mice. (A) Gating strategy. The proportion of live B-cells (CD19+) that express the germinal center marker GL7 and plasmablast marker CD138 were quantified in groups of FV-infected and uninfected B6 *Apobec3*$^+$ and B6 *Apobec3*-deficient F_1 mice (n=6 mice for each group). (B) Germinal center B cells and plasmablasts in the spleen. Higher levels of GL7+ B cells (*Upper* panel) and CD138+ plasmablasts (*Lower* panel) were detected in FV-infected B6 *Apobec3*$^+$ F_1 mice compared to B6 *Apobec3*-deficient F_1 mice. Mean values were subjected to a 2-tailed Student's *t*-test; **, $p<0.01$. Error bars correspond to the standard error of the mean.

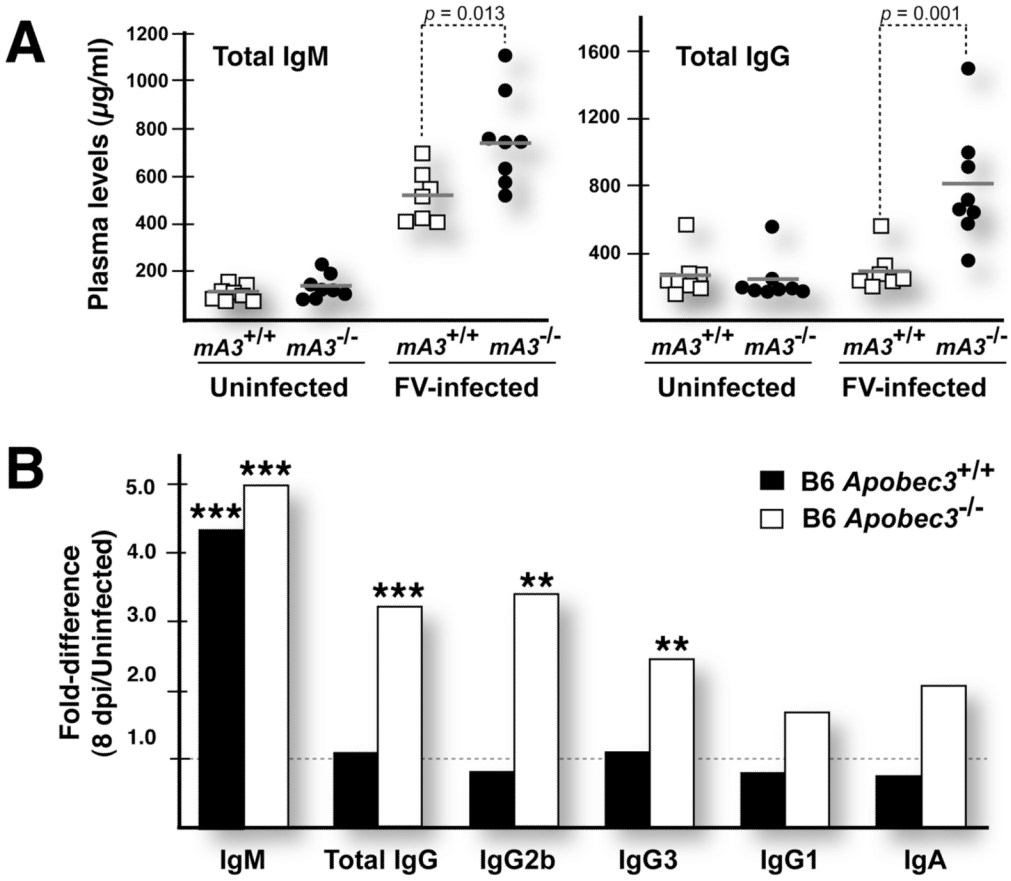

Figure 7.

Hypergammaglobulinemia in FV-infected B6 Apobec3-deficient mice. (A) Total IgM and IgG titers in FV infected mice. Plasma titers of IgM and IgG were determined in acutely infected and uninfected wild-type (□) and Apobec3-deficient (●) B6 mice. Horizontal gray bars correspond to mean levels. Data were analyzed and *p* values calculated using a 2-tailed Student's *t*-test. In the upper panel, mouse *Apobec3* was abbreviated as '*mA3*'. Acute FV infection increased IgM titers in both strains of mice, but total IgG levels were selectively upregulated in Apobec3-deficient mice. (B) Induction of IgG subclasses during acute FV infection. "Fold-difference" corresponds to the mean immunoglobulin levels of FV infected (n=7–8) divided by the mean levels in uninfected mice (n=8). The difference in immunoglobulin titers between the infected and uninfected mice were subjected to a 2-tailed Student's *t*-test. ***, $p<0.001$; **, $p<0.01$. Selective upregulation of total IgG in Apobec3-deficient mice was likely due to induced levels of IgG2b and IgG3.

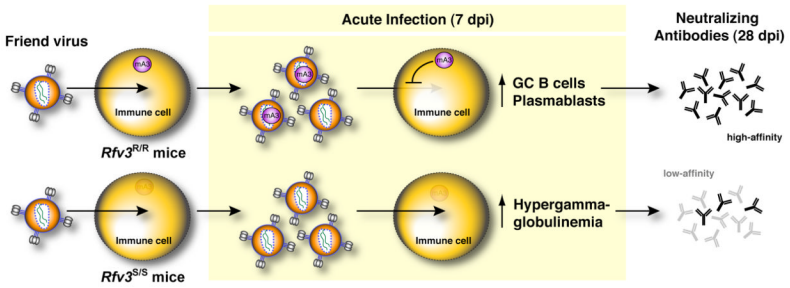

Figure 8.

Working model for how Apobec3 influences the FV-specific neutralizing antibody response. Acute FV infection of multiple immune cells (erythroid, B, T and myeloid) which express Apobec3 (*upper* row) results in the release of noninfectious particles containing Apobec3 that in next round of infection display reduced infectivity for target cells. At the same time, these Apobec3+ viral particles could prime virus-specific antibody responses by presenting native envelope trimers. Reduced pathology in the presence of viral antigen results in the induction of germinal center B cells and plasmablasts that eventually translate to the development of high-affinity virus-specific antibodies. In Apobec3-deficient/*Rfv3* susceptible mice (*lower* row), uncontrolled FV replication in B cells, and possibly other immune cells, results in aberrant polyclonal B cell activation as highlighted by hypergammaglobulinemia and suppressed B cell responses. This translates to delayed affinity maturation of virus-specific antibodies. In this model, we hypothesize that high-affinity envelope-specific antibodies contribute significantly to a potent neutralizing antibody response.

TABLE I

FV infection of (B6 Apobec3+ x A.BY) F_1 and mice at 7 dpi.

Cell Subpopulation	Cohort[a]	Marker	WT[b]	KO[b]	*p* value[c]
BONE MARROW					
Erythroid	1	Ter119+	3.83 ± 1.33	33.37 ± 4.43	0.0004
	2	Ter119+	2.20 ± 0.45	25.65 ± 6.82	0.0108
	3	Ter119+	2.37 ± 0.81	25.65 ± 2.70	0.0002
B cells	1	B220+	1.43 ± 0.31	9.93 ± 1.88	0.0037
	2	CD19+	2.34 ± 0.23	17.50 ± 4.57	0.0128
	3	CD19+	2.11 ± 0.22	8.24 ± 0.99	0.0012
Myeloid	1	CD11b+	0.53 ± 0.11	2.52 ± 0.76	0.0335
	3	CD11b+	0.37 ± 0.12	2.94 ± 0.57	0.0058
Granulocytes	1	Gr-1+	1.03 ± 0.20	4.51 ± 1.00	0.0128
	2	Gr-1+	0.64 ± 0.12	3.00 ± 0.88	0.0321
	3	Gr-1+	0.17 ± 0.04	1.54 ± 0.25	0.0024
T-cells	2	CD3+	1.84 ± 0.19	7.15 ± 1.66	0.0150
SPLEEN					
Erythroid	1	Ter119+	12.01 ± 3.69	26.93 ± 5.13	0.0379
	3	Ter119+	13.87 ± 3.47	33.47 ± 1.72	0.0013
	4	Ter119+	4.26 ± 0.95	18.59 ± 4.19	0.0178
B-cells	1	CD19+	4.16 ± 0.78	6.52 ± 1.47	0.1896
	3	CD19+	5.06 ± 1.12	12.32 ± 1.09	0.0009
	4	B220+	1.87 ± 0.50	7.33 ± 1.26	0.0057
T-cells	1	CD3+	2.70 ± 0.58	5.85 ± 0.79	0.0084
	3	CD3+	2.81 ± 0.46	6.80 ± 1.00	0.0084
	4	CD3+	1.02 ± 0.13	2.78 ± 0.29	0.0008
Myeloid	1	CD11b+	3.46 ± 0.85	7.81 ± 1.24	0.0149
	3	CD11b+	4.56 ± 0.98	10.09 ± 0.93	0.0022
	4	CD11b+	1.99 ± 0.40	8.73 ± 1.25	0.0021

[a] FV infections were performed on 4 separate cohorts of (B6 *Apobec3*$^{+/+}$ x A.BY) (WT) and (B6 *Apobec3*$^{-/-}$ x A.BY) (KO) F_1 mice. The sample sizes are as follows. Cohort 1: WT=7, KO=7; Cohort 2: WT=8, KO=8; Cohort 3: WT=6, KO=6; Cohort 4: WT=7, KO=6.

[b] Entries correspond to the mean FV^+ cells ± standard error of the mean of (B6 *Apobec3*$^{+/+}$ x A.BY) F_1 (WT) and (B6 *Apobec3*$^{-/-}$ x A.BY) (KO) F_1 mice, respectively.

[c] *p*-values were computed using a 2-tailed Student's *t*-test.